



ELSEVIER

Contents lists available at ScienceDirect

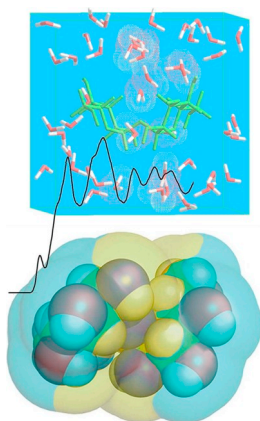
## Biophysical Chemistry

journal homepage: [www.elsevier.com/locate/biophyschem](http://www.elsevier.com/locate/biophyschem)

## Hydrodynamic volume of trehalose and its water uptake mechanism

Nader Sakhaee<sup>a,b,\*</sup>, Sahar Sakhaee<sup>c</sup>, Ahmad Takallou<sup>b</sup>, Akbar Mobaraki<sup>b</sup>, Mina Maddah<sup>b</sup>, Reza Moshrefi<sup>b</sup><sup>a</sup> Harris-Stowe State University Saint Louis, MO 63108, United States<sup>b</sup> KN Toosi University, Tehran, Iran<sup>c</sup> Islamic Azad University, Mashhad Branch, Iran

## GRAPHICAL ABSTRACT



## ARTICLE INFO

## Keywords:

Trehalose  
Hydrodynamic volume  
Semicircular heterogeneities  
Radial distribution functions  
Trehalose conformational switch  
Bound waters  
Coordination water

## ABSTRACT

Trehalose ability to preserve water in biology has spawned research on this special disaccharide and its solutions. Trehalose unlike any other disaccharide, tend to mix with almost any amount of water. In water, Trehalose forms a hydrodynamic volume with bound waters (both coordination water and semicircular heterogeneities), capable of perturbing the very nature of normal bulk water. Switching of the two major conformational forms, defined by their helicities (*i*, *i*-H<sub>2</sub>O with lower helicity and *ii*, *ii*-H<sub>2</sub>O with higher helicity), were closely examined, using DFT/B3LYP- 6-311 + G\*\* level of theory, along with molecular dynamic (MD) calculations in aqueous media. Patterns in radial distribution functions (RDF) confirmed semicircular heterogeneities, including spines of water (rows of slow water molecules), in Trehalose hydration shell. Dynamics of Trehalose conformational switch and its coordination water are coupled to dynamics of these spines of water, which are themselves coupled to dynamics of the rest of Trehalose hydration shell waters. Like seamless cogwheels such energy cascade links the upstream slow dynamics of spines to the downstream collective bulk water dynamics. This lubricates Trehalose conformational switch through coordination water uptake, for which we proposed a mechanism here. We show how the coupling between Trehalose and bound waters in its hydrodynamic volume encompass both function and dynamic of the molecule and its hydration shell. Further simulations are needed to

\* Corresponding author at: Harris-Stowe State University Saint Louis, MO 63108, United States.

E-mail address: [SakhaeeN@Hssu.edu](mailto:SakhaeeN@Hssu.edu) (N. Sakhaee).

<https://doi.org/10.1016/j.bpc.2019.03.002>

Received 1 March 2019; Received in revised form 30 March 2019; Accepted 31 March 2019

Available online 02 April 2019

0301-4622/ © 2019 Elsevier B.V. All rights reserved.

see how this ability is related to the evading and percolating nature of cryoprotectant water, also reported for the self-coordinating jelly behavior of biological water.

## 1. Introduction

### 1.1. Trehalose and its aqueous solutions

Trehalose is the most stable and interesting of all disaccharides with a rich biochemistry yet to be discovered. It's the only disaccharide used as a very potent fuel in flying insects, and is widely used among both plant and animal life to preserve precious water in either dry or freezing conditions. Perhaps the key to understand the peculiarities of Trehalose lies in its intricate relation with the ubiquitous bio solvent, water. Trehalose is a non-reducing sugar with a considerable PH tolerance range (3.5–10). The glycosidic  $\alpha(1\text{--}1)$   $\alpha$  bond is responsible for the profound stability of this molecule. The energy released upon breaking  $\alpha(1\text{--}1)\alpha$  bond in Trehalose is twice as much that for glycosidic bond in starch [1].

Biological importance of sugars can only be addressed in the context of their aqueous solutions. Trehalose solutions are interesting because of the sugar's ability to grip a tight hold on water molecules in its solvation shells [2]. Trehalose is not only used as a potent fuel in flying insects but also helps create a sort of homeostasis in insect's body fluid thanks to its cryogenic properties. This unique feature accounts for Trehalose tendency to preserve precious water in dry and other dehydrating conditions. Resurrection plants in deserts can tolerate long droughts thanks to their ability to produce large amounts of Trehalose in the ephemeral and short periods of torrential rains. Trehalose has also been found in the body fluids of aquatic plants and some shrimps, where it helps prevent dehydration due to inverse osmotic pressure of sea water. Water in Trehalose aqueous solutions re-assembles into a more tightly packed cryoprotectant state with decreased tetrahedral order [1] and thus making it more like a super cooled water reluctant to freeze [3] with more of a lubricant behavior [4] just like the water in biological cavities [5–8] of macromolecules such as the coordination water in DNA's minor groove [9,10].

Here we try to present a clearer picture of Trehalose hydrodynamic volume. Dynamics of the bound water in Trehalose hydration shell are coupled to its conformational switch. With both ab initio and MD computations we trace out a mechanism for Trehalose coordination water uptake, which falls in line with heterogeneities found in MD simulations.

While Maltose and lactose tend to form some aggregates in concentrated solutions, for Trehalose there is just a slight change in the number of molecules in its solvation shell [11]. Cryoprotectant effectiveness of Trehalose solutions are reported [12,13], in line with evidence on decreased tetrahedral order of surrounding water molecules in its sugary solution. Cryoprotectant water is more of a self-coordinating jelly that percolates into limited confinements available to its molecules, compared to normally expanding enveloping jelly that acts as a potent solvent [3,14–16].

Solvation shell dynamics of sugar solutes are in tight relation with water's  $\alpha$ -relaxation. Slow  $\alpha$ -relaxation occurs in temperature range starting off the boundary of non-ergodic solid regime of water with perfect tetrahedral order (ice), to the transient water cage regime defining near freezing water and then extending into fast the  $\alpha$ -relaxation with rattling water cage which eventually collapse into liquid like regime, through ballistic motions. This lower limit glassy transition of bulk water is reported to be around  $-135^\circ\text{C}$  for most sugary solutions and based on this criteria our model temperature range is chosen. Trehalose is known to have reduced the surface tension of water through engaging water molecules to itself and thus resists freezing far much better than Sucrose solutions [1,2,17–19]. The first solvent shell

around Trehalose is an assembly of at least 47 to 50 water molecules [20]. This makes the most concentrated solution of interest to be a 60% w/w mixture. With this we found an ambient concentration to run MD computations.

## 2. Methods

All energy computations were done at DFT/6–311 + G(d,p) level of theory [21,22]. Conformational search were done only for dihedrals along the  $C_1\text{--}O_\alpha\text{--}C_1'$  moiety (or the typical  $\varphi$  and  $\varphi'$ ) [23]. Structures were then subjected to water coordination optimizations [24,25] through  $O_\alpha$  of Trehalose. Finally solvation energies were run, using Cosmo-polarized continuum model (CPCM), by using Gaussian g09 [26–30] package to get an initial guess of the mechanism and a cast of starting structures for ensuing molecular dynamic (MD) computations.

All of the MD simulations were carried out with the GROMACS 4.5.6 package [31]. A modified force field based on AMBER 03 force field [32] was adopted for Trehalose in water. Each starting structure was placed in a cubic box. In all cases, the minimum distance from any solute atom to the edge of the box was 12 Å. The boxes were then filled with TIP3P water molecules [33]. In all MD simulations, periodic boundary conditions were applied in all directions. The temperature was kept in by coupling 230, 265 and 310 k with a Nose-Hoover thermostat for the initial production runs of 20 ns [34,35]. To maintain the systems at constant pressure of 1 bar, a Parrinello–Rahman barostat [36] was applied. The particle mesh Ewald (PME) algorithm [37] was applied for long-range electrostatic interactions while SHAKE algorithm [38] was used to constrain all bonds involving hydrogen atoms. The cutoff distance for van der Waals interactions was set to 10 Å. The leapfrog algorithm with time step of 2 fs was utilized to integrate the equations of motion. First, 5000 step steepest descent minimization with position restraints of 1000 kJmol<sup>-1</sup> nm<sup>-2</sup> on the water molecules was performed, followed by the 5000 step unrestrained minimizations using the steepest descent and conjugate gradient methods were carried out. Then, two 200 ps equilibration phase were performed under NVT and NPT ensemble respectively. Then, production runs for each T were carried out for 20 ns under conditions of constant pressure and temperature. And, finally production runs of 30 ns with applied T-gradients were carried out. In the second ten nanosecond systems were heated to 270 K (starting from 230 K) followed by equilibration. These runs provided exquisite fluctuation patterns on  $\varphi / \varphi'$ , which enabled us to propose a mechanism for coordination water uptake. Radial Distribution Functions (RDFs) gave more insight into the nature of heterogeneities in Trehalose hydrodynamic volume.

## 3. Results and discussion

Trehalose is symmetric molecule that can have a range of different helicities (two major conformers are shown in Fig. 1). If the skeletal sugar rings face straight towards each other helicity is zero (with  $C_5$  Symmetry for the rings). The helicity of the molecule grows up with rings facing a bit way in a skewed orientation (and the two rings now assume a lower symmetry of  $C_2$  (Fig. 1 Bottom). There are a few improper dihedrals that can be used to address Trehalose conformers. Two major conformers were found, namely *i* and *ii*, with lower and higher helicity, +15 and +55 respectively (Fig. 1 Top), where the helicity is defined by the improper dihedral  $C_4\text{--}C_1\text{--}C_1'\text{--}C_4'$ , indicating the rotation of two rings with respect to each other. To analyze the results of MD simulations, conventional  $\varphi / \psi$  labels [23] are used, however this notion is reduced to  $\varphi / \varphi'$  form as the two dihedrals in Trehalose are equal with  $\varphi$  being  $H_1\text{--}C_1\text{--}O_\alpha\text{--}C_1'$  and  $\varphi'$  being  $H_1'\text{--}C_1'\text{--}O_\alpha\text{--}C_1$

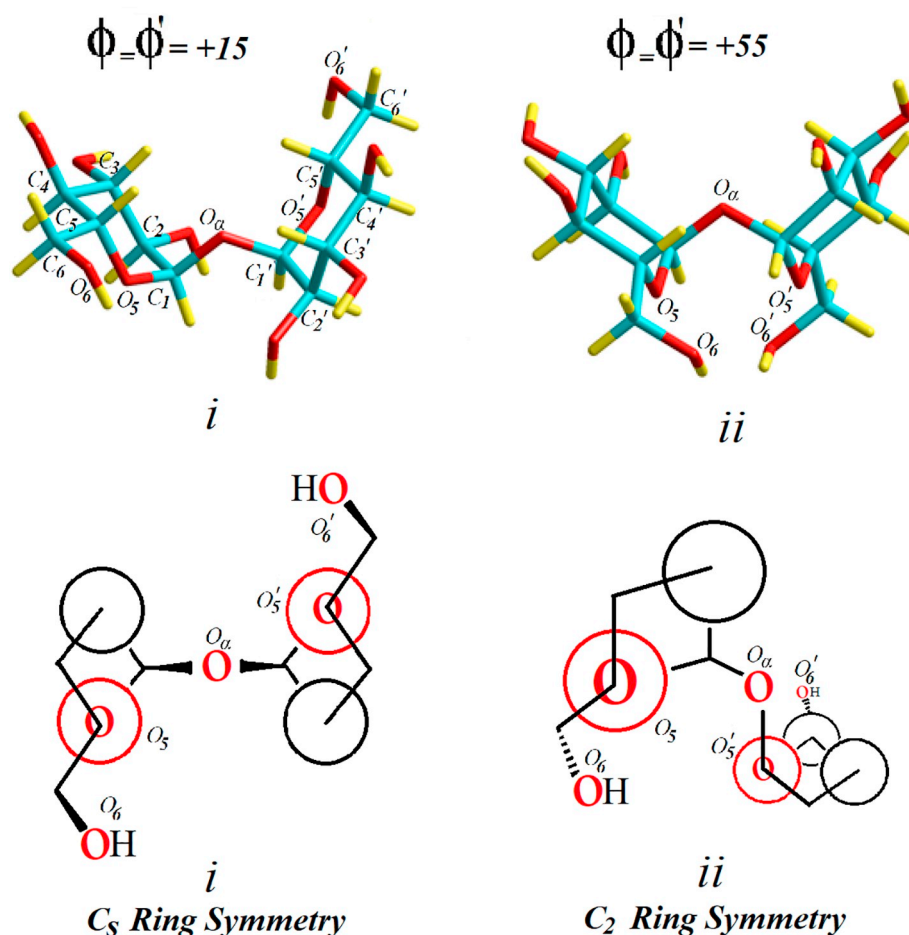


Fig. 1. Top: Tube model of the two major Trehalose conformers showing the numbering. Bottom: Corresponding Newman projection models for Trehalose conformers representing the symmetry of skeletal sugar rings.

respectively (Fig. 1 Top).

Initial MD Runs on Trehalose molecules alone, showed two distinct conformational regions pertaining to *i* and *ii* conformers. It also revealed an inherent switching behavior for Trehalose (Fig. 2 Top Right). The two major conformers for Trehalose, each with or without coordination water, make up a total of four species referred to as *i*, *i*-H<sub>2</sub>O, *ii* and *ii*-H<sub>2</sub>O hereafter. Subsequent MD runs were done on each of these four species with a final 30 ns production run including a T-gradient (230–270 K from 9 to 19 ns), called the heating phase. The detailed trajectories of  $\phi / \phi'$  dihedrals are given and discussed in the SI. Here the two less stable, of prime importance to coordination water uptake mechanism, are discussed (Fig. 2 Top left). Both *ii*-H<sub>2</sub>O and *i* show a sort of stable  $\phi / \phi'$  dihedral before the heating phase (See SI Fig. S1), while *ii* and *i*-H<sub>2</sub>O clearly shows wavy patterns of  $\phi / \phi'$  dihedral with random jump lines even before the heating phase (Fig. 2 Top left). Thus, *ii* and *i*-H<sub>2</sub>O show a stronger tendency to undergo conformational switches. Moreover, upon heating an earlier transition is seen in both *i*-H<sub>2</sub>O and *ii*, which confirms the previously mentioned instability of these species. Species *ii*-H<sub>2</sub>O shows a clear stability reluctant to give up its coordination water, even upon heating, compared to other species (See SI Fig. S1). Finally, one can see both conformers will reach a dynamic equilibrium after the heating phase with major *ii*-H<sub>2</sub>O and *i* as the two dominant species. This dynamic equilibrium (See SI on RDF patterns) is reached after the heating phase, no matter which of the four species one starts with.

Lining up the result of energy computations for all these Species, along with their solvation energies, using Cosmo-polarized continuum model (CPCM) (Table 1), we can propose the coordination water uptake

mechanism. Such mechanism will start with stable *i* conformer without any coordination water, it goes to an unstable conformer *i*-H<sub>2</sub>O upon water absorption. This unstable hydrated form can now either lose its coordination water to go back to the stable initial form (*i*), or it can kinetically lose its coordination water to go to conformer *ii* which readily and strongly absorbs water to form the very stable conformer *ii*-H<sub>2</sub>O form. Thus in this mechanism the (*i*-H<sub>2</sub>O  $\leftrightarrow$  *ii*) is the rate determining step for coordination. It can readily populate these two mobile flexible components *i*-H<sub>2</sub>O or *ii*, if cooled or heated respectively (Fig. 2 Bottom).

It seems like the discussed mechanism involves a sequence of grab-release-grab for the coordination water uptake and its worth to look back and ask why such species like *i*-H<sub>2</sub>O are even involved in the mechanism (couldn't it have just been *i* to *ii* to *ii*-H<sub>2</sub>O). The simplest yet tricky answer is that the coordination water is needed if one wishes to either wind or unwind the curl in Trehalose. Just a look at the RDF patterns will illustrate the issue. Finally the full scope of hydrodynamic volume of Trehalose and its bound waters being either a coordination water or a spine of water is explored to unravel the underpinnings of the proposed mechanism. Detailed of RDF patterns are elaborated in SI. Here only the key features shown by RDF patterns are discussed. One such feature is the exchange rate for coordination water. While *ii*-H<sub>2</sub>O shows the smallest exchange rate for coordination water, *i*-H<sub>2</sub>O shows the highest exchange rate. This implies that while *ii*-H<sub>2</sub>O is reluctant to release its coordination water, *i*-H<sub>2</sub>O is sort of eager to eject it. One other striking difference between the two coordinated forms is the compactness and order of their hydrodynamic volume. While *ii*-H<sub>2</sub>O shows an intricately compact state with a nano-sized hydrodynamic

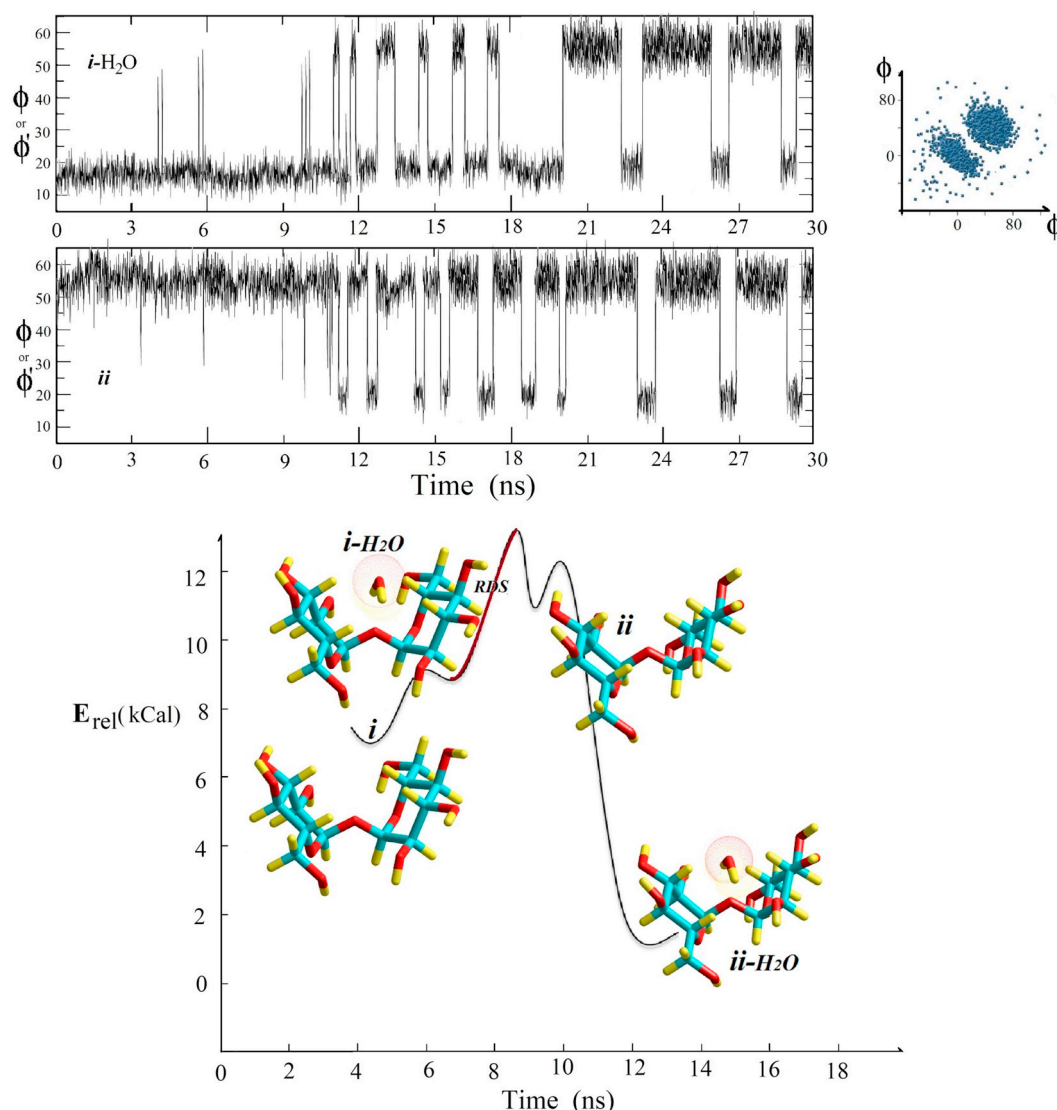


**Fig. 2.** Top Right: Population of the major conformers resulting from MD simulation of Trehalose alone based on  $\phi / \phi'$  dihedrals. Top Left: Conformational switch of Trehalose in water upon heating, shown here for fast equilibrating, more flexible species *ii* and *i-H<sub>2</sub>O*. Bottom: Proposed mechanism for coordination water uptake by Trehalose in aqueous media.

cluster [39], (See SI on RDF patterns page S6) the *i-H<sub>2</sub>O* shows a rather spherical featureless hydration shell with a loosely held coordination water. With these we can now look at the bound waters (coordination water and spines) in Trehalose hydrodynamic volume and attribute a role to bound waters regarding the conformational switch.

Helical and even chiral spines of water have also been reported for DNA minor groove. DNA minor groove is in fact host to some water molecules with weirdly slow dynamics (reorientation times of up to 85 ps). While bulk water and most hydration shell waters are retarded by both hydrophobic and polar phosphate groups, a few water molecules tend to snug fit into DNA's minor groove not only to stabilize DNA conformations but also lubricating its unwinding processes [9]. Our MD computations in the case of Trehalose clearly showed signs of this heterogeneities (assemblies of [Trehalose (H<sub>2</sub>O)<sub>n</sub>]<sub>m</sub>, 8 < n < 12, m = 1,2) in hydration shells with distinct semicircular strings of waters referred to as spines. Results has revealed different patterns of such heterogeneities, unique to each conformer (Fig. 3). Hydration energies reported in (Table 1) are computed not for the solvation of Trehalose conformers themselves but rather for the solvation of each of the four species *i*, *i-H<sub>2</sub>O*, *ii*, *ii-H<sub>2</sub>O* as presented in (Fig. 3). close examination of these four species also shows that the helicity of flexible species *ii* and *i*

H<sub>2</sub>O are a little bit different from the parent equilibrium species *ii-H<sub>2</sub>O* and *i* respectively (see Fig. 3). Interestingly with more helicity the hydration energy grows and the structure needs more stabilization through solvation effects. When isolated the conformer *i* is more stable than conformer *ii* of Trehalose. This is because the compactness of the more helical conformer brings oxygen atoms closer together and there's no bound water to compensate for that. Upon conformational switch from the less helical *i* conformer to the more helical *ii* conformer the distance of hydroxyl groups O<sub>6</sub>O<sub>6'</sub> goes from 8.78 Å to 7.36 Å and the ring oxygen O<sub>5</sub>O<sub>5'</sub> distance goes from 4.57 Å to 3.49 Å. Conformer *ii*

**Table 1**

Electronic energies relative to the energy of *ii-H<sub>2</sub>O* as reference for Trehalose conformers (E), along with their aqueous solvation energies reported as (E<sub>hyd</sub>) (Using CPCM model).

conf/cmp	E(kcal)	-E <sub>hyd</sub> (kcal)	E <sub>tot</sub> (kcal)
<i>i</i>	8.7	2.3	6.4
<i>ii</i>	16.4	5.7	11.7
<i>i-H<sub>2</sub>O</i>	9.7	0.5	9.2
<i>ii-H<sub>2</sub>O</i>	1.5	1.5	0

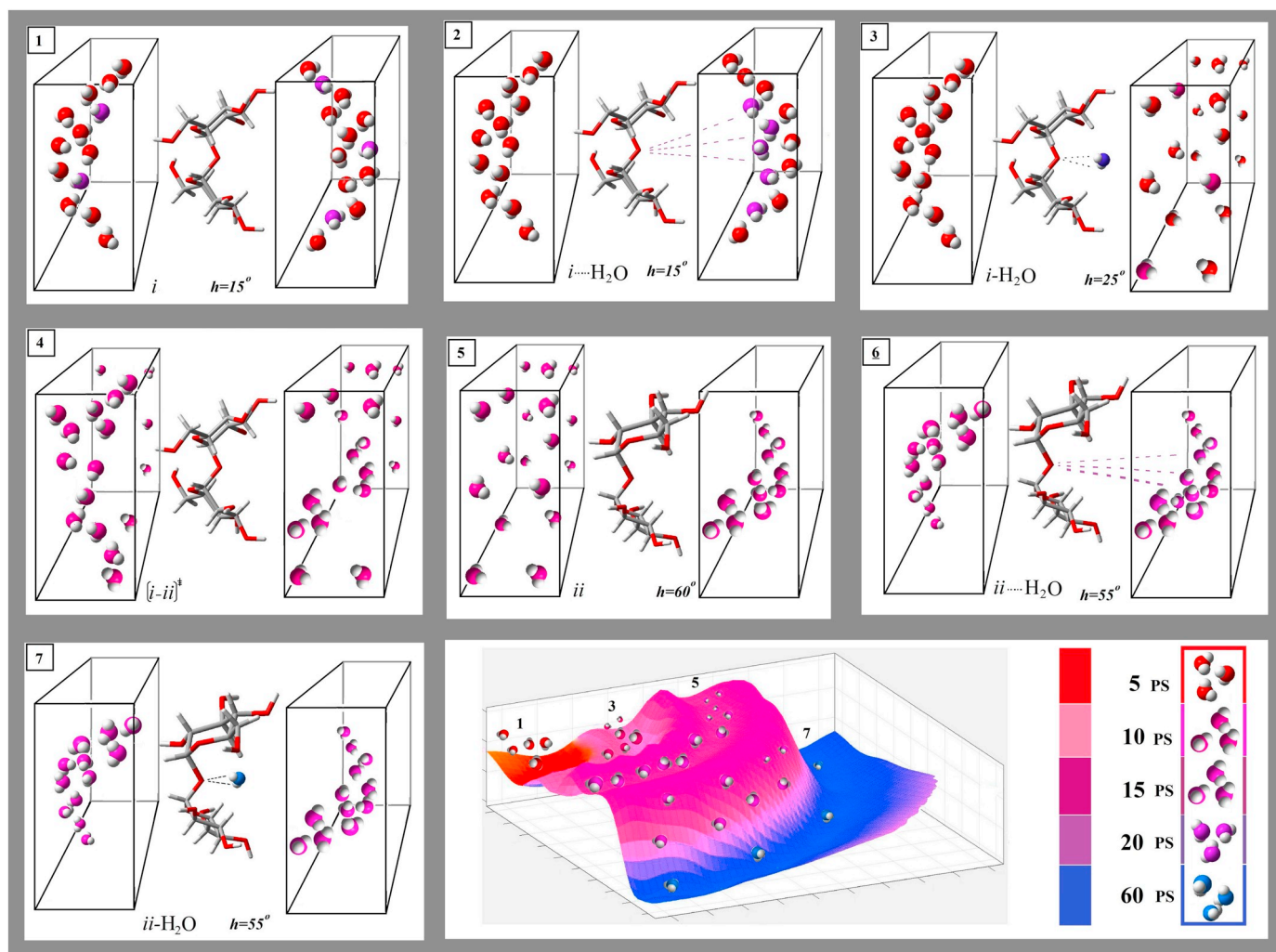


**Fig. 3.** Coupled dynamics of bound waters (Spines and coordination water) and Trehalose conformers. The letter “h” represents helicity in local Trehalose conformer. Boxes showing a uniform distribution of water are not spines, but rather meant to show their collapse and rebirth in Trehalose hydrodynamic volume. Coloring is used to separate the waters based on their dynamics. A range of 20 to 60 ps time range was used as shown in the legend to address such differences in water dynamics. The energy cascade, shown on the legend, makes the connection between the bound water dynamics and energy flow in the proposed mechanism. Note that, it is not a conformational energy landscape, rather it's a cascade of water dynamics as coupled to Trehalose conformational switch).

also creates a narrow inner groove like cavity which is perfect to accommodate a coordination water.

We can now go back to hydrodynamic volume of Trehalose and interrogate the role played by the bound waters (Fig. 3). Species *i* represents a Trehalose with two eclipsed spines with a rather high affinity to grasp a coordination water from the frontal spine. However, upon intake of the coordination water the frontal spine collapses, and *i*-H<sub>2</sub>O is formed. The *i*-H<sub>2</sub>O species has an awkward fit for the coordination water, its coordination site is not a snug fit one. Thus there is a high tendency to either eject it in a thermodynamic kick out process, or the coordination water will kinetically tweak the Trehalose molecule itself to undergo a conformational switch and thus forming a narrow groove in doing so. When the coordination water kinetically tweaks the Trehalose, it will slowly move out and rejoined by a group of other water molecules to make up a spine which is tightly held by the narrow groove of conformer *ii*. Species *ii* has a narrow unstable groove with a tight grip for the frontal spine. If one of these water molecules falls into this narrow groove it fits so tightly that not only stabilizes the otherwise unstable conformer but also drags in another spine in staggered configuration relative to the existing frontal one. This staggered configuration of spines locks in and sort of hides out the narrow groove and its

snug fit coordination water, and thus giving *ii*-H<sub>2</sub>O its enormous stability.

#### 4. Conclusions

In this paper, it's been tried to show how the effect of Trehalose on water is rather much more of a two-way path deeply affecting both solvent shells and solute's conformers. Solvation shells can play a central role in the conformational change of Trehalose in aqueous solutions. The two processes are coupled and synchronized through coordination water dynamics. The water uptake mechanism shows how coordination water trigger conformational switch to Conformer *ii*. The latter is the more stable form in aqueous medium and has a characteristic inner groove that is stabilized by spines of waters, like those reported for the minor groove of DNA. A mechanism is proposed for coordination water uptake in Trehalose. In the big picture Trehalose conformers, its coordination water and spines of water form an energy cascade like cogwheels geared to one another, driving the folding and unfolding of this beautiful disaccharide. These new findings should shed light on the importance of hydration shells in carbohydrate chemistry. We believe that slow dynamic water molecules which are

woven into the cavities of biomolecules can help them smoothly flow in a conformational landscape essential to their function and bioactivity.

## Acknowledgement

Acknowledgment is made to the National Science Foundation for cyber-infrastructure to access the facilities of the Pittsburgh supercomputing center (NSF grant #: 1541435), as well as the XSESE startup allocation (CTS170029/Lu) to support the research. The authors also thank Dr. Yun Lu and Southern Illinois University Edwardsville Chemistry Department Computational facilities.

## Appendix A. Supplementary data

Supplementary data to this article can be found online at <https://doi.org/10.1016/j.bpc.2019.03.002>.

## References

- [1] S. Paul, S. Paul, Molecular insights into the role of aqueous Trehalose solution on temperature-induced protein denaturation, *J. Phys. Chem. B* 119 (4) (2015) 1598–1610.
- [2] A. Magno, P. Gallo, Understanding the mechanisms of bioprotection: a comparative study of aqueous solutions of Trehalose and maltose upon supercooling, *J. Phys. Chem. Lett.* 2 (9) (2011) 977–982.
- [3] O. Kirichek, A. Soper, B. Dzyuba, W. Holt, Segregated water observed in a putative fish embryo cryopreservative, *R. Soc. Open Sci.* 3 (3) (2016) 150655.
- [4] R. Lemieux, A. Pavia, J. Martin, K. Watanabe, Solvation effects on conformational equilibria. Studies related to the conformational properties of 2-methoxytetrahydropyran and related methyl glycopyranosides, *Can. J. Chem.* 47 (23) (1969) 4427–4439.
- [5] S.K. Pal, J. Peon, B. Bagchi, A.H. Zewail, Biological water: femtosecond dynamics of macromolecular hydration, *J. Phys. Chem. B* 106 (48) (2002) 12376–12395.
- [6] D. Wang, S. Liu, B.J. Trummer, C. Deng, A. Wang, Carbohydrate microarrays for the recognition of cross-reactive molecular markers of microbes and host cells, *Nat. Biotechnol.* 20 (3) (2002) 275.
- [7] G. Ashwell, A.G. Morell, The role of surface carbohydrates in the hepatic recognition and transport of circulating glycoproteins, *Adv. Enzymol. Relat. Areas Mol. Biol.* 41 (1974) 99–128.
- [8] A. Takada, K. Ohmori, T. Yoneda, K. Tsuyuoka, A. Hasegawa, M. Kiso, R. Kannagi, Contribution of carbohydrate antigens sialyl Lewis x and sialyl Lewis X to adhesion of human cancer cells to vascular endothelium, *Cancer Res.* 53 (2) (1993) 354–361.
- [9] M.L. McDermott, H. Vanselow, S.A. Corcelli, P.B. Petersen, DNA's chiral spine of hydration, *ACS Central Sci.* 3 (7) (2017) 708–714.
- [10] S.K. Pal, L. Zhao, A.H. Zewail, Water at DNA surfaces: ultrafast dynamics in minor groove recognition, *Proc. Natl. Acad. Sci.* 100 (14) (2003) 8113–8118.
- [11] S. Magazu, P. Migliardo, A. Musolino, M. Sciortino,  $\alpha$ ,  $\alpha$ -Trehalose – water solutions. I. Hydration phenomena and anomalies in the acoustic properties, *J. Phys. Chem. B* 101 (13) (1997) 2348–2351.
- [12] P.B. Conrad, J.J. de Pablo, Computer simulation of the cryoprotectant disaccharide  $\alpha$ ,  $\alpha$ -Trehalose in aqueous solution, *J. Phys. Chem. A* 103 (20) (1999) 4049–4055.
- [13] E.M.-E. Aboagla, T. Terada, Trehalose-enhanced fluidity of the goat sperm membrane and its protection during freezing, *Biol. Reprod.* 69 (4) (2003) 1245–1250.
- [14] L. Lanzi, M. Carlà, L. Lanzi, C.M. Gambi, A new insight on the dynamics of sodium dodecyl sulfate aqueous micellar solutions by dielectric spectroscopy, *J. Colloid Interface Sci.* 330 (1) (2009) 156–162.
- [15] C. Branca, S. Magazu, G. Maisano, P. Migliardo, Anomalous cryoprotective effectiveness of Trehalose: Raman scattering evidences, *J. Chem. Phys.* 111 (1) (1999) 281–287.
- [16] J. Malsam, A. Aksan, Hydrogen bonding and kinetic/thermodynamic transitions of aqueous Trehalose solutions at cryogenic temperatures, *J. Phys. Chem. B* 113 (19) (2009) 6792–6799.
- [17] T. Sei, T. Gonda, Y. Arima, Growth rate and morphology of ice crystals growing in a solution of Trehalose and water, *J. Cryst. Growth* 240 (1–2) (2002) 218–229.
- [18] N. Ekdawi-Sever, J.J. de Pablo, E. Feick, E. von Meerwall, Diffusion of sucrose and  $\alpha$ ,  $\alpha$ -Trehalose in aqueous solutions, *J. Phys. Chem. A* 107 (6) (2003) 936–943.
- [19] P.D. Orford, R. Parker, S.G. Ring, Aspects of the glass transition behaviour of mixtures of carbohydrates of low molecular weight, *Carbohydr. Res.* 196 (1990) 11–18.
- [20] L.R. Winther, J. Qvist, B. Halle, Hydration and mobility of Trehalose in aqueous solution, *J. Phys. Chem. B* 116 (30) (2012) 9196–9207.
- [21] L. Goerigk, S. Grimme, Efficient and accurate double-hybrid-meta-GGA density functionals evaluation with the extended GMTKN30 database for General Main group thermochemistry, kinetics, and noncovalent interactions, *J. Chem. Theory Comput.* 7 (2) (2010) 291–309.
- [22] Y. Shao, L.F. Molnar, Y. Jung, J. Kusmann, C. Ochsenfeld, S.T. Brown, A.T. Gilbert, L.V. Slipchenko, S.V. Levchenko, D.P. O'Neill, Advances in methods and algorithms in a modern quantum chemistry program package, *Phys. Chem. Chem. Phys.* 8 (27) (2006) 3172–3191.
- [23] D. Kony, W. Damm, S. Stoll, P.H. Hünenberger, Explicit-solvent molecular dynamics simulations of the  $\beta$  (1 $\rightarrow$ 3)- and  $\beta$  (1 $\rightarrow$ 6)-linked disaccharides  $\beta$ -laminarabiose and  $\beta$ -gentiobiose in water, *J. Phys. Chem. B* 108 (18) (2004) 5815–5826.
- [24] H.P. Hratchian, P.V. Parandekar, K. Raghavachari, M.J. Frisch, T. Vreven, QM: QM electronic embedding using Mulliken atomic charges: energies and analytic gradients in an ONIOM framework, *J. Chem. Phys.* 128 (3) (2008) 034107.
- [25] A. Klamt, V. Jonas, Treatment of the outlying charge in continuum solvation models, *J. Chem. Phys.* 105 (22) (1996) 9972–9981.
- [26] Y. Takano, K. Houk, Benchmarking the conductor-like polarizable continuum model (CPCM) for aqueous solvation free energies of neutral and ionic organic molecules, *J. Chem. Theory Comput.* 1 (1) (2005) 70–77.
- [27] A.D. French, G.P. Johnson, C.J. Cramer, G.I. Csonka, Conformational analysis of cellobiose by electronic structure theories, *Carbohydr. Res.* 350 (2012) 68–76.
- [28] H.-Y. Cao, D.-H. Si, Q. Tang, X.-F. Zheng, C. Hao, Electronic structures and solvent effects of unsymmetrical neo-confused Porphyrin: DFT and TDDFT-IEFPCM investigations, *Comput. Theor. Chem.* 1081 (2016 April 1) 18–24.
- [29] D.J. Giesen, M.Z. Gu, C.J. Cramer, D.G. Truhlar, A universal organic solvation model, *J. Organomet. Chem.* 61 (25) (1996) 8720–8721.
- [30] M. Frisch, G. Trucks, H. Schlegel, G. Scuseria, M. Robb, J. Cheeseman, G. Scalmani, V. Barone, B. Mennucci, Petersson; Gaussian 09, Revision B. 01, Gaussian, Inc, Wallingford, CT, 2009.
- [31] B. Hess, C. Kutzner, D. Van Der Spoel, E. Lindahl, GROMACS 4: algorithms for highly efficient, load-balanced, and scalable molecular simulation, *J. Chem. Theory Comput.* 4 (3) (2008) 435–447.
- [32] Y. Duan, C. Wu, S. Chowdhury, M.C. Lee, G. Xiong, W. Zhang, R. Yang, P. Cieplak, R. Luo, T. Lee, A point-charge force field for molecular mechanics simulations of proteins based on condensed-phase quantum mechanical calculations, *J. Comput. Chem.* 24 (16) (2003) 1999–2012.
- [33] W.L. Jorgensen, J. Chandrasekhar, J.D. Madura, R.W. Impey, M.L. Klein, Comparison of simple potential functions for simulating liquid water, *J. Chem. Phys.* 79 (2) (1983) 926–935.
- [34] S. Nosé, A unified formulation of the constant temperature molecular dynamics methods, *J. Chem. Phys.* 81 (1) (1984) 511–519.
- [35] W.G. Hoover, Canonical dynamics: equilibrium phase-space distributions, *Phys. Rev. A* 31 (3) (1985) 1695.
- [36] M. Parrinello, A. Rahman, Polymorphic transitions in single crystals: a new molecular dynamics method, *J. Appl. Phys.* 52 (12) (1981) 7182–7190.
- [37] U. Essmann, L. Perera, M.L. Berkowitz, T. Darden, H. Lee, L.G. Pedersen, A smooth particle mesh Ewald method, *J. Chem. Phys.* 103 (19) (1995) 8577–8593.
- [38] J.-P. Ryckaert, G. Cicotti, H.J. Berendsen, Numerical integration of the cartesian equations of motion of a system with constraints: molecular dynamics of n-alkanes, *J. Comput. Phys.* 23 (3) (1977) 327–341.
- [39] R.B. Jadrich, J.A. Bollinger, B.A. Lindquist, T.M. Truskett, Equilibrium cluster fluids: pair interactions via inverse design, *Soft Matter* 11 (48) (2015) 9342–9354.